Available at www.sciencedirect.com

ScienceDirect

journal homepage: www.elsevier.com/locate/he

Influence of rare earth content on electrode kinetics in Misch metal-based AB_5 MH alloys – Cyclic voltammetric investigations

M.V. Ananth[a,*], M. Ganesan[a], N.G. Renganathan[a], S. Lakshmi[b]

[a]Ni–MH Section, Electrochemical Energy Sources Division, Central Electrochemical Research Institute, Alagappapuram, Karaikudi 630 006, India

[b]Department of Chemistry, Dhanalakshmi Srinivasan College of Arts & Science for Women, Perambalur 621 212, India

ARTICLE INFO

Article history:
Received 31 October 2007
Received in revised form
6 August 2008
Accepted 24 September 2008
Available online 21 November 2008

Keywords:
Hydrogen storage alloy
Lanthanum/cerium ratio
X-ray florescence
Cyclic voltammetry
Electrokinetic properties

ABSTRACT

The influence of lanthanum/cerium ratio (0.42–14.14) in Misch metal (Mm)-based AB_5-type hydrogen storage alloys has been investigated. The samples were subjected to X-ray florescence (XRF) and cyclic voltammetry (CV) studies. The metal hydride electrodes were assembled, and their discharge capacity was determined. These alloys delivered discharge capacity between 118 and 266 mAh/g. CV investigations threw light on charge-transfer reactions at the electrode/electrolyte interface and hydrogen surface coverage capacity. The CV parameters in general indicate that the battery activity increases with lanthanum/cerium ratio. At low lanthanum/cerium values, the discharge reactions proceed at potentials that are more negative. Furthermore, electrochemical reversibility of the hydrogen absorption–desorption on the alloy surface is enhanced at optimum lanthanum/cerium ratio as revealed by decreasing values of peak separation. The slopes of graphical plots of I_{peak} (anodic) vs. $\nu^{1/2}$ for the fully charged samples reverse direction at very high lanthanum/cerium values. The results suggest that the discharge plateau is optimum at lanthanum/cerium ratio around 12.

1. Introduction

Ni–MH batteries are being widely used in various portable electronic devices, electric hand tools, hybrid electric vehicles, etc [1]. Rare earth-based AB_5-type alloys and Zr-based Laves phase alloys have realised successful commercialisation as Ni–MH secondary cell negative materials. Nowadays, many commercial Ni–MH batteries contain AB_5-type alloys as negative electrode materials [2]. Investigations on the AB_5-type rare earth-based hydrogen storage alloys are in progress for further improvement in electrochemical characteristics and reduction in production cost. With this view in mind, replacements are being made elsewhere with relatively cheap Misch metal – a combination of selected rare earths. The Misch metal formulations can be made with different permutations and combinations within permissible limits for obtaining better electrochemical performance. Amongst the various factors that can affect the electrochemical hydrogen storage, lanthanum/cerium ratio is a significant one. Already investigations done at our laboratory have demonstrated the

* *Corresponding author*. Fax: +91 4565 227713
E-mail address: mvananth@rediffmail.com (M.V. Ananth).

0360-3199/$ – see front matter © 2008 International Association for Hydrogen Energy. Published by Elsevier Ltd. All rights reserved.
doi:10.1016/j.ijhydene.2008.09.072

dependence of maximum capacity on lanthanum/cerium ratio [3]. The lanthanum/cerium ratio exercised significant effect on the performance and best performing samples had this value around 12. However, detailed studies have not been made so far with respect to the influence of lanthanum/cerium ratio on the electrochemical performance of these alloys in Ni–MH batteries.

$LaNi_5$ alloy, the original material, which forms the basis of AB_5-type hydrogen storage alloys, has been extensively studied [4,5] ever since Van Vucht [6] reported his work in 1970. Many researchers have considered partial substitution of selective elements for lanthanum and nickel as an effective way for improving the overall performances of $LaNi_5$ [7–18]. During the past decade, reports of studies on lanthanum replacement were fewer than that on nickel replacement. Previous reports about the A-site replacement of AB_5-type alloy mainly focused on cerium element substitution for lanthanum. This is because of their relatively higher content in the rare earth element family. However, different researchers have drawn different conclusions. Taking the activation property of alloy as an example, some researchers reported that increase of cerium content in AB_5-type alloy can prolong the activation process [7], but other researchers have drawn the conclusion that activation property was almost independent of cerium content in A-site [9]. Therefore, the effects of the cerium content in the alloys are complicated and a clear picture is yet to emerge. It is worth mentioning that effect of lanthanum/magnesium ratio on the structure and electrochemical properties of $La_xMg_{3-x}Ni_9$ ($x = 1.6$–2.2) ternary alloys has been investigated [19]. Also the effects of manganese substitution for nickel on the structural and electrochemical properties of the $La_{0.7}Mg_{0.3}Ni_{3.4-x}Co_{0.6}Mn_x$ ($x = 0.0$, 0.2, 0.3, 0.4, 0.5) hydrogen storage alloys have been systematically studied [20,21].

Hence in the present study, six compositions of Mm (Ni Co Al Mn)$_5$ hydrogen storage alloys with wide variations in rare earth content (La/Ce = 0.42–14.14) in Mm part have been investigated for rare earth content with XRF and electrode kinetics by CV.

2. Experimental

Hydrogen storage alloys were prepared by button arc melting followed by necessary treatments at our collaborating laboratory DMRL, Hyderabad, India. The purity of all elements was above 99 wt.%. The annealed alloys were mechanically crushed into powder (<75 μm). XRF measurements were performed on a HORIBA XRF Analyser in non-standard mode for determining lanthanum/cerium ratio.

The working electrodes used for electrochemical measurements were prepared with 0.5 g of the alloy. The alloy was thoroughly mixed with PTFE binder to form a paste and was then applied over either sides of nickel foam substrate. Subsequently compaction was done at a pressure of 3 tones for 1 min followed by heat treatment at 125 °C for 1 h. The undesirable areas of the electrode were sealed with epoxy resin in order to insulate them from electrolyte. The negative electrodes were soaked in KOH solution for 3 h prior to measurements. The counter electrode was sintered nickel hydroxide electrode and the reference electrode engaged was a homemade Hg/HgO (6 mol L^{-1} KOH) electrode. The electrolyte was 6 mol L^{-1} KOH solution, which was prepared with KOH (Guaranteed Reagent) and ultra pure water (resistivity > 18 MΩ cm). After each electrochemical measurement, the cavity of working electrode was disposed by ultrasonic treatment in 1 mol L^{-1} HCl solution. Cyclic voltammetric measurements were done in the voltage range −0.2 to −1.2 V with respect to Hg/HgO reference electrodes at different sweep rates varying from 5 to 500 mV/s (25 ± 2 °C). Such measurements were performed in a classical three-electrode cell on an electrochemical working station (Autolab PGSTAT30 potentiostat–galvanostat).

For cell assembly and capacity evaluation, 1 g of MH alloy was thoroughly mixed with 20% KS44 Graphite powder, 10% Carbonyl Nickel and 10% Silver Oxide. The electrodes were prepared as detailed earlier. The geometric area of the negative electrode was 1 cm^2 and the thickness was 1.5 mm. For charge–discharge cycle experiments, negative electrode was sandwiched between two sintered {NiOOH/Ni(OH)$_2$} positive electrodes using a 'Scimat' separator. The electrolyte was a 6 mol L^{-1} KOH solution. Discharge capacity was measured using automatic Bitrode LCN equipment (30 °C). The assembled cells were discharged at C_5 rate to a discharge cut-off potential of 1 V.

3. Results and discussion

3.1. XRF analysis and battery experiments

The lanthanum and cerium contents of the samples were determined with XRF. The discharge capacities were determined by assembling Ni–MH cells and performing battery charge/discharge experiments. The results are presented in Table 1. It is evident that the battery activity increases up to

Table 1 – Influence of rare earth content (lanthanum/cerium) on performance of MH alloys

Alloy	Lanthanum content (%)	Cerium content (%)	(Lanthanum/cerium) ratio	Maximum capacity (mAh/g)
A	7.96	19.15	0.42	172.00
B	13.28	20.63	0.64	188.00
C	11.71	14.75	0.79	190.00
D	36.34	3.83	9.49	223.00
E	36.57	3.14	11.65	266.00
F	32.24	2.28	14.14	118.00

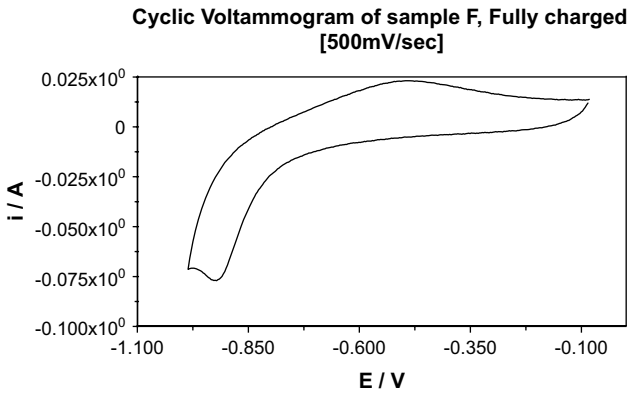

Fig. 1 – Typical cyclic voltammogram of a fully charged MH alloy (sample F).

a lanthanum/cerium ratio of about 12 and decreases thereafter.

3.2. *Structure and cell parameters*

The XRD patterns of some of the investigated MH alloys have been already reported by us [3]. A typically monoclinic crystalline structure was assigned. Also, development of additional phases was observed in samples with lanthanum/cerium ratio around 0.5. Literature survey has indicated that with the increase of cerium content in the A-site of the alloy, the parameter *a* and cell volume decreased remarkably, but the parameter *c* increased slightly [9]. Two different contributions of the element cerium valence (by Ce^{3+}, Ce^{4+}) were traceable in the alloys [22–24], and about 30% of cerium element was at a valence of four. Therefore, the average radius of cerium atoms in AB_5-type alloy is 1.73 Å, which is

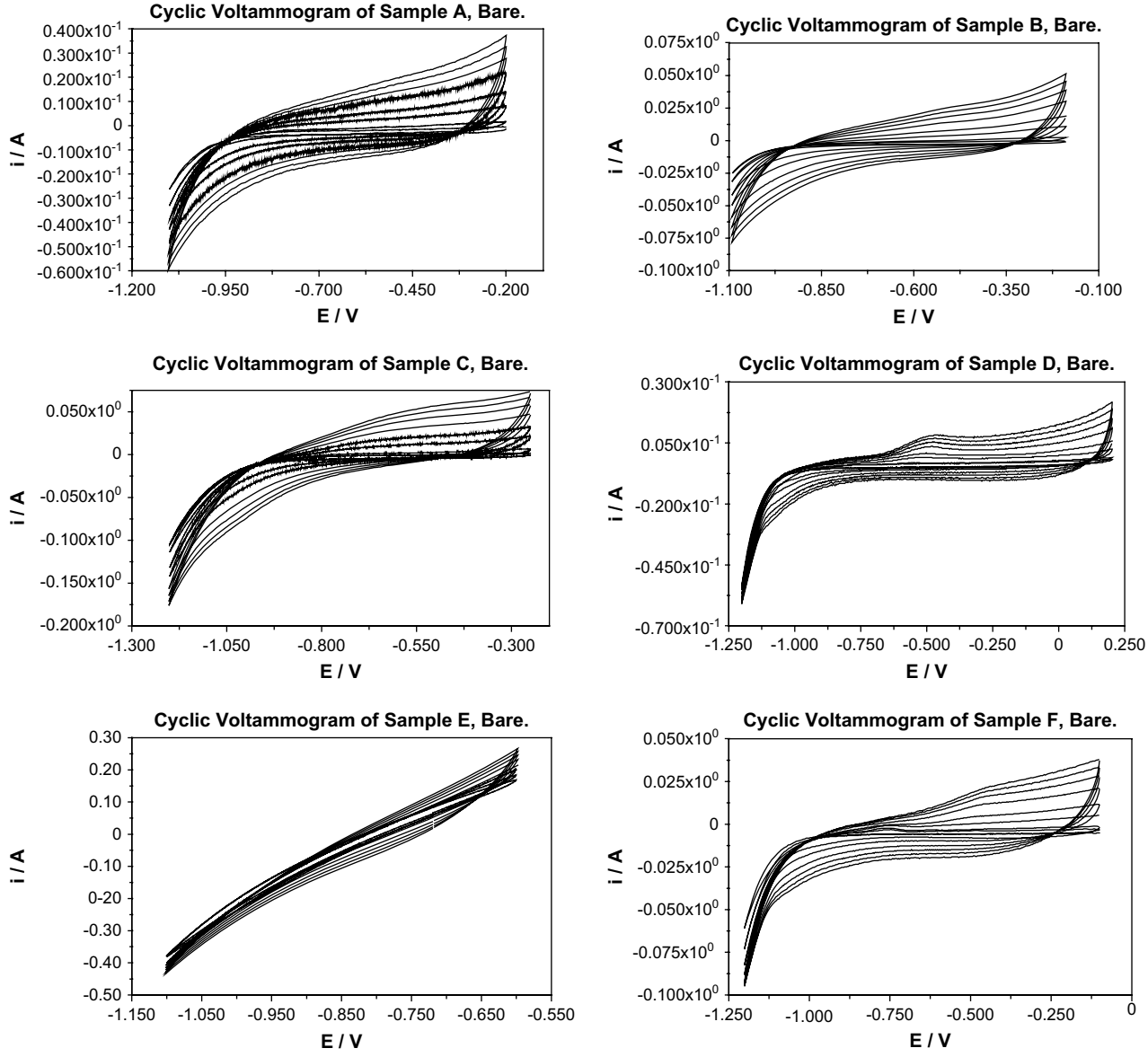

Fig. 2 – Cyclic voltammograms of bare uncharged metal hydride alloys at different scan rates varying from 5 to 500 mV/s.

smaller than that of the lanthanum element (about 1.87 Å). This is the reason for the decrease in cell volume with increasing cerium content. These results have confirmed that the replacement of cerium for lanthanum in the alloy is successful, and this forms the basis for the comparative evaluation of the electrochemical properties of the partially substituted alloys.

3.3. *Cyclic voltammetric measurements*

Fig. 1 shows a typical cyclic voltammogram of the investigated MH alloy F. The electrode potential was scanned from −1.10 to −0.1 V vs Hg/HgO (6 mol L^{-1} KOH solution) at a scan rate of 500 mV/s. The observed anodic and cathodic peaks provide detailed information about the discharge and charge processes of the alloy respectively. Since the charging process of the alloy is often affected by hydrogen evolution on the alloy surface, the cathodic peak widens and is inconspicuous in many cases as seen in other samples. Hence, only the discharge process of the alloy is chosen for the comparative study.

The cyclic voltammograms of the investigated bare alloys are illustrated separately in Fig. 2. The anodic peak observed is due to the oxidation of the desorbed hydrogen atoms at the surface. The anodic peak current increases and anodic peak potential shifts towards positive direction with scan rate. The cyclic voltammetric patterns change with lanthanum/cerium ratio thereby confirming its influence on electrokinetic properties. This is in support of our earlier findings [3] wherein we observed an orderly influence of lanthanum/cerium ratio on the crystalline structure.

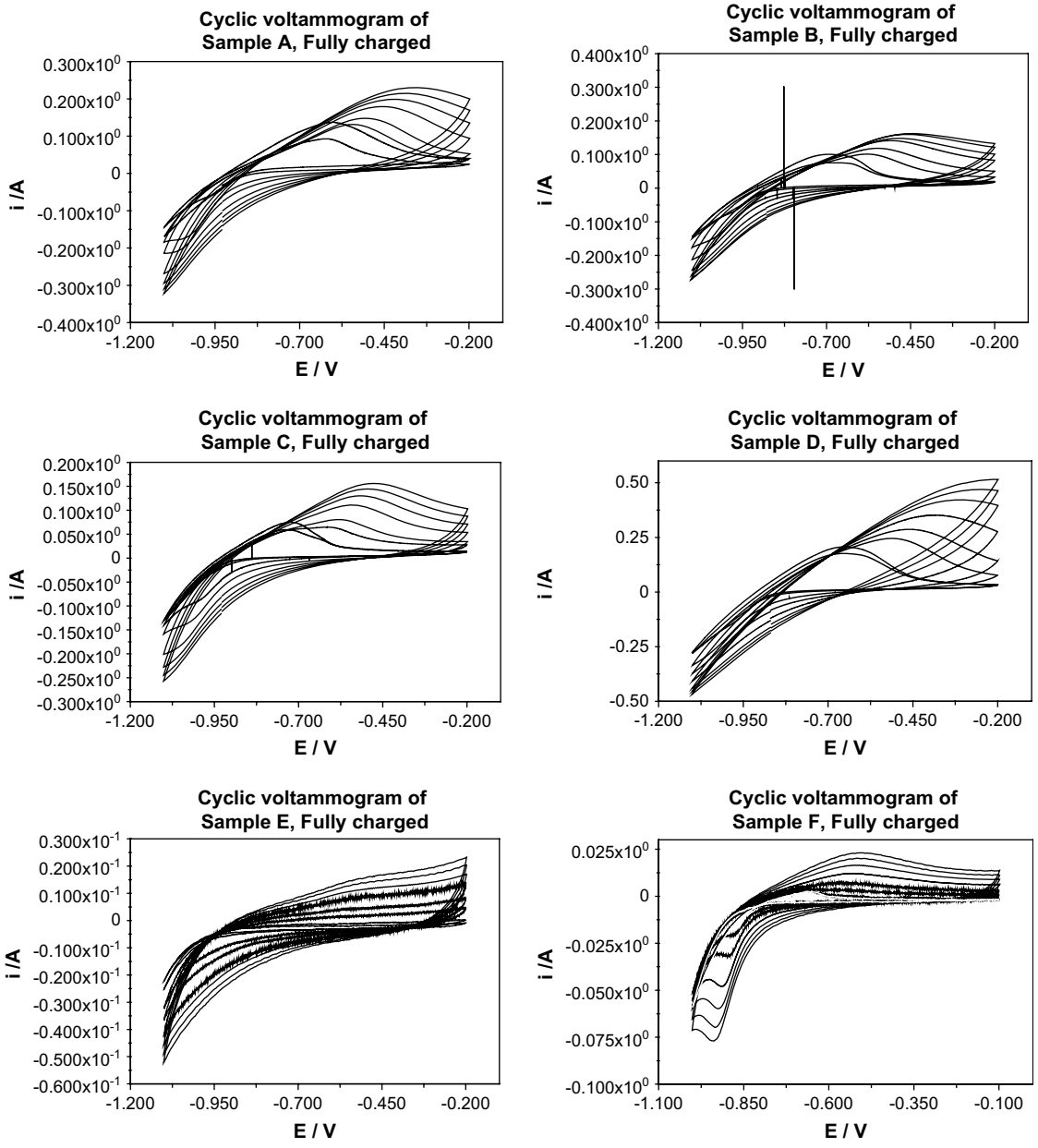

Fig. 3 – Cyclic voltammograms of fully charged metal hydride alloys at different scan rates varying from 5 to 500 mV/s.

The micropolarization measurements have indicated that the electrochemical kinetic properties of MH alloys improve with increasing state of charge, due to the increase of the electrocatalytic activation of the surface and the increase of the hydrogen diffusivity in the bulk alloy [25]. The exchange current density, the polarization resistance and the equilibrium potential are important parameters that characterize the electrochemical kinetic properties of metal hydride electrode. These parameters depend on the characteristics of the electrode reactions such as temperature, state of charge, surface modification and life cycles. As such, the cyclic voltammograms of the fully charged MH alloys obtained are depicted in Fig. 3. The CV patterns change with lanthanum/cerium ratio thereby confirming its influence on electrokinetic properties. The results are in accordance with battery capacity experiments.

Since these samples were fully charged, several useful parameters were derived from the cyclic voltammograms recorded at a scan rate of 5 mV/s and are tabulated in Table 2. The reversibility of the electrochemical reaction increases with lanthanum/cerium ratio as seen from decreasing values of peak separation. The cyclic voltammetric parameters in general indicate that the battery activity increases with lanthanum/cerium ratio as revealed by peak area and other parameters. A deep analysis of the CV curves at different scan rates confirms the excellent recyclability of the alloys. The potential sweeps were done at −1.2 V as lower limit and −0.1 V as upper limit in most cases. An adsorbate zone of H reduced species near HER potential occurs in this plot when the potential is in the cathodic direction. In the anodic direction of the potential sweep, an oxidizing zone of H species exist at potentials higher than −0.8 V. An explicit redox couple is observed in these figures.

Thus, cyclic voltammetry is a powerful tool for investigating the adsorption phenomenon of various electrochemical systems. As far as metal hydride electrode is concerned, the process involved in the hydride electrode has two main steps i.e., a surface charge-transfer process and a solid phase hydrogen diffusion process. Hydrogen adsorption is not explicitly visible as a peak in the cathode direction. In some cases a step has appeared. Except in initial cases wherein some shift in peak potentials occurred, the values are relatively stable. The peak height shows a regular decrease which however intensifies at very high lanthanum/cerium ratio. The peak area shows a gradual decrease up to lanthanum/cerium ratio value of around 10 and then exhibits a speedy recovery.

Table 3 – Determination of transfer co-efficient α for MH alloys

Alloy	Lanthanum content (%)	Cerium content (%)	(Lanthanum/cerium) ratio	α
A	7.96	19.15	0.42	0.1210
B	13.28	20.63	0.64	0.1192
C	11.71	14.75	0.79	0.1216
D	36.34	3.83	9.49	0.2161
E	36.57	3.14	11.65	0.1221
F	32.24	2.28	14.14	–

The anodic peak is due to the oxidation of the desorbed hydrogen atoms at the surface. Anodic peak current generally increases with scan rate. Anodic peak potential shifted to positive direction with scan rate. Anodic peak potential E_{ap} of these compounds has a linear dependence with log(ν). Results indicate that the investigated alloys form irreversible systems. Slopes of these curves yield α for the reaction, described in the following equation, and they are given in Table 3.

$$dE_{ap}/d\log(\upsilon) = 2.3RT/2\alpha nF$$

The graphical plots of I_{peak} (anodic) vs. $\nu^{1/2}$ for the fully charged samples are shown in Fig. 4. At low lanthanum/cerium ratios, the slopes are mostly linear. At further high lanthanum/cerium values, the slope emerges and its direction reverses at very high lanthanum/cerium values. Thus, these graphical plots indicate some trend with increasing lanthanum/cerium values.

3.3.1. *Activation properties of the alloys with varied rare earth content*

In multi-cycle process of the alloy, the anodic current of CV curve increased with increasing the cycle number at the same potential during the initial cycling. This behavior corresponds to the activation process of the alloy [26]. Since Q_A expresses the discharge capacity, the appearance of the maximum value of the integrated anodic charge $Q_{A(max)}$ indicates the completion of the activation process of the alloy. The alloys with different A-site component require different cycle numbers to finish the activation process. Our results are generally in line with that of Adzic et al. [7] that the increase of the cerium

Table 2 – Determination of cyclic voltammetric parameters of MH alloys

Sample	Lanthanum/cerium ratio	E/V min (V)	E/V max (V)	Peak separation (V)	Peak height	Peak area (c)	Peak width at half maximum	Q_+ (c)	Q_- (c)
A	0.42	−1.1	−0.605	0.495	0.1066	6.664	0.305	13.45	−6.194
B	0.64	−1.1	−0.695	0.405	0.0908	5.192	0.264	8.029	−5.462
C	0.79	−1.1	−0.725	0.375	0.0676	3.186	0.213	4.964	−4.186
D	9.49	−1.0	−0.653	0.347	0.0190	1.210	0.303	16.11	−11.03
E	11.65	−1.1	−0.647	0.453	0.0787	5.052	0.303	5.754	−5.645
F[a]	14.14	−1.0	−0.662	0.338	0.0038	5.670	0.102	0.033	−2.315

a Multiple peaks are seen.

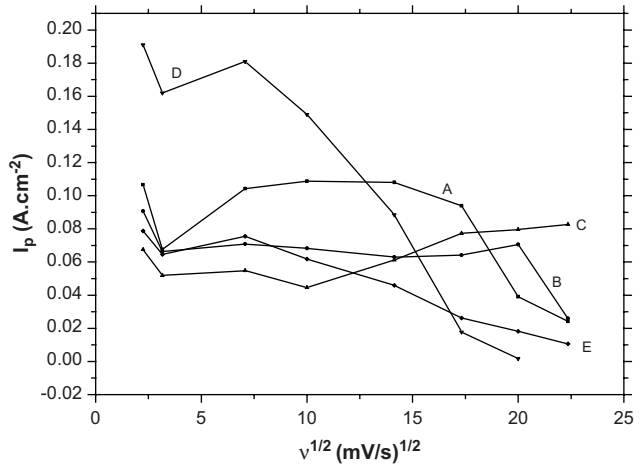

Fig. 4 – The graphical plots of I_{peak} (anodic) vs. $\nu^{1/2}$ for the fully charged samples.

content decreased the activation property of MH alloys. In some cases the alloys required only about 6–8 cycles for completion of activation and the activation cycle number was almost independent of cerium content as per the study by Yuan et al. [9]. These differences in conclusion could have resulted from the different ways of preparation of the working electrode and the structural factor of alloy with different B-site composition. Furthermore, the activation process leads to cleavage of alloy particles.

3.3.2. *Comparison of stable CV of MH alloys*

Fig. 3 shows the stable CV of MH alloys. It is evident that the shapes of CV curves are not identical instead differ from each other depending on the rare earth content. The valuable information obtained is listed below:

(1) The cathodic peak appears clearly only in sample F with very high lanthanum/cerium ratio. It gradually widens and is inconspicuous in other samples with decreasing lanthanum/cerium ratio.
(2) The peak potential of the discharge process shifted towards negative direction in alloys with high cerium content (low lanthanum/cerium values). This is in line with the results of Zuxian Tan et al. [27]. The results obtained are displayed in Table 4.
(3) The anodic peak current or the maximum current output ability of the alloy is best at lanthanum/cerium ratio of 9.49. Otherwise, the results are in accordance with Zuxian Tan et al. [27].

From the results observed, two conclusions can be drawn: (1) the hydrogen storage alloy is discharged at more negative potential in alloys with high cerium content (low lanthanum/cerium values) and hence it can be deduced that the discharge plateau of Ni–MH battery can be improved by using the alloy with optimum lanthanum/cerium ratio around 12. (2) The electrochemical reversibility of the hydrogen absorption–desorption on the alloy surface is enhanced with lanthanum/cerium ratio near 12.

The cathodic peak appears more and more distinct and the peak potential shifts to values that are more positive with increase in lanthanum/cerium ratio. The peak potential of the discharge process shifts towards negative direction on increasing the lanthanum content (Table 4). With decrease in lanthanum/cerium ratio, the variation trend of the anodic current becomes smaller and smaller as the potential is shifted towards positive direction in the potential region from −0.4 to −0.3 V.

The anodic peak current occurring at around −700 mV vs. Hg/HgO is due to the oxidation of the hydrogen adsorbed in the alloy. The anodic peak current values are indicative of the electrocatalytic activity of the hydrogen electrode for hydrogen oxidation. Partial replacement of cerium by lanthanum causes remarkable changes in anodic peak current. This suggests that the electrocatalytic activity of the hydrogen electrode for hydrogen oxidation varies due to substitution.

3.3.3. *Comparison of electrochemical reactivity of MH alloy*

In general, electron transfer on the alloy surface on the left half branch of the CV curve controls the anodic reaction. Therefore, the reaction current in this potential region is a measure of the interfacial electrochemical activity at the corresponding potential *E*. This could actually result from the combination of two factors, i.e., the increased kinetic force, which leads to higher discharge current, and the decreased residual capacity in the bulk alloy at potential *E*. Therefore, the electrochemical activity on the alloy surface is best at the optimum lanthanum/cerium ratio around 12 in MH alloy.

4. Conclusions

Investigations on the electrokinetics of six AB_5 MH alloy formulations with lanthanum/cerium ratio in the A part varying from 0.42 to 14.14 were carried out in 6 mol L^{-1} KOH for use as negative electrode material in Ni–MH battery. A plastic bonding procedure over nickel foam was adopted for the preparation of the electrodes. Based on the results we can

Table 4 – Influence of rare earth content on discharge potential and anodic peak current of MH alloys

Alloy	Lanthanum content (%)	Cerium content (%)	(Lanthanum/cerium) ratio	E_{peak} (anodic) at 5 mV/s (V)	I_{peak} (anodic) at 5 mV/s (A cm^{-2})
A	7.96	19.15	0.42	−0.605	0.107
B	13.28	20.63	0.64	−0.695	0.091
C	11.71	14.75	0.79	−0.725	0.068
D	36.34	3.83	9.49	−0.659	0.191
E	36.57	3.14	11.65	−0.647	0.079

conclude that the charge-transfer mechanism of the MH alloys are influenced by lanthanum/cerium ratio in the A part. Furthermore, significant changes in CV patterns arise due to differences in rare earth content and the battery activity increases with lanthanum/cerium ratio.

Acknowledgement

The authors thank the Director, CECRI, Karaikudi for encouragement and permission to publish this work. Thanks are to MNES, New Delhi for sanctioning a Grant-In-Aid project on 'Development of Advanced Ni–MH Battery fitted Electric Cycle and Field Studies' in which the above work has been done. The authors also thank Dr. G. Balachandran, DMRL, Hyderabad, India for preparing the metal alloys. Thanks are due to M. Raju and K. Manimaran, scientists of Ni–MH section, CECRI for giving support. One of the authors, SL, thanks the Director, CECRI for permission to carry out her MSc project work and Dr. MVA for guidance.

REFERENCES

[1] Zhang XB, Sun DZ, Yin WY, Chai YJ, Zhao MS. Effect of Mn content on the structure and electrochemical characteristics of $La_{0.7}Mg_{0.3}Ni_{2.975-x}Co_{0.525}Mn_x$ ($x = 0$–0.4) hydrogen storage alloys. Electrochim Acta 2005;50(14):2911–8.

[2] Yin Wenya, Zhao Minshou. Structure and electrochemical characteristics of $TiV_{1.1}Mn_{0.9}Ni_x$ ($x = 0.1$–0.7) alloys. Electrochim Acta 2007;52(7):2723–8.

[3] Ananth MV, Raju M, Manimaran K, Balachandran G, Nair LM. Influence of rare earth content on Mm-based AB_5 metal hydride alloys for Ni–MH batteries – an X-ray fluorescence study. J Power Sources 2007;167(1):228–33.

[4] Van Mal HH, Buschow KHJ, Miedeme AR. Hydrogen absorption in $LaNi_5$ and related compounds: experimental observations and their explanation. J Less-Common Met 1974;35(1):65–76.

[5] Goodell PD, Rudman PS. Hydriding and dehydriding rates of the $LaNi_5$–H system. J Less-Common Met 1983;89(1):117–25.

[6] Van Vucht JHN, Kuijpers FA, Bruning HCAM. Reversible room-temperature absorption of large quantities hydrogen by intermetallic compounds. Philips Res Rep Suppl 1970; 25(2):133–40.

[7] Adzic GD, Lohnson JR, Reilly JJ, McBreen J, Mukerjee S. Cerium content and cycle life of multicomponent AB_5 hydride electrodes. J Electrochem Soc 1995;142(10):3429–33.

[8] Ye Hui, Xia Baojia, Wu Wenquan, Du Ke, Zhang Hong. Effect of rare earth composition on the high-rate capability and low-temperature capacity of AB_5-type hydrogen storage alloys. J Power Sources 2002;111(1):145–51.

[9] Yuan Xianxia, Liu Han-San, Ma Zi-Feng, Xu Naixin. Characteristics of $LaNi_5$-based hydrogen storage alloys modified by partial substituting La for Ce. J Alloys Compd 2003;359(1–2):300–6.

[10] Sakai Tetsuo, Oguro Keisuke, Miyamura Hiroshi, Kuriyama Nobuhiro, Kato Akihiko, Ishikawa Hiroshi, et al. Some factors affecting the cycle lives of $LaNi_5$-based alloy electrodes of hydrogen batteries. J Less-Common Met 1990; 161(2):193–202.

[11] Willems JJG, Buschow KHJ. From permanent magnets to rechargeable hydride electrodes. J Less-Common Met 1987; 129:13–30.

[12] Sakai Tetsuo, Miyamura Hiroshi, Kuriyama Nobuhiro, Kato Akihiko, Oguro Keisuke, Ishikawa Hiroshi, et al. The influence of small amounts of added elements on various anode performance characteristics for $LaNi_{2.5}Co_{2.5}$-based alloys. J Less-Common Met 1990;159:127–39.

[13] Liu Yongfeng, Pan Hongge, Gao Mingxia, Miao He, Lei Yongquan, Wang Qidong. Function of Al on the cycling behavior of the La–Mg–Ni–Co-type alloy electrodes. Int J Hydrogen Energy 2008;33(1):124–33.

[14] Shih RJ, Oliver Su Y, Perng TP. Self-supported electrodes made of $LaNi_{4.25}Al_{0.15}Co_{0.5}V_{0.1}$ and Ag or Ni for hydrogenation. Int J Hydrogen Energy 2006;31(12):1716–20.

[15] Wei Xuedong, Tang Rui, Liu Yongning, Zhang Peng, Yu Guang, Zhu Jiewu. Effect of small amounts of Li on microstructures and electrochemical properties of non-stoichiometric low-Co AB_5-type alloys. Int J Hydrogen Energy 2006;31(10):1365–71.

[16] Pan Hongge, Liu Yongfeng, Gao Mingxia, Zhu Yunfeng, Lei Yongquan. The structural and electrochemical properties of $La_{0.7}Mg_{0.3}(Ni_{0.85}Co_{0.15})_x$ ($x = 3.0$–5.0) hydrogen storage alloys. Int J Hydrogen Energy 2003;28(11):1219–28.

[17] Seo Chan-Yeol, Choi Seung-Jun, Choi Jeon, Park Choong-Nyeon, Lee Jai-Young. Effect of vanadium content on electrochemical properties of La-based AB_5-type metal hydride electrodes. Int J Hydrogen Energy 2003;28(9):967–75.

[18] Seo Chan-Yeol, Choi Seung-Jun, Choi Jeon, Park Choong-Nyeon, Lee PS, Lee Jai-Young. Effect of Ti and Zr additions on the characteristics of AB_5-type hydride electrode for Ni–MH secondary battery. Int J Hydrogen Energy 2003;28(3):317–27.

[19] Liao B, Lei YQ, Chen LX, Lu GL, Pan HG, Wang QD. Effect of the La/Mg ratio on the structure and electrochemical properties of $La_xMg_{3-x}Ni_9$ ($x = 1.6$–2.2) hydrogen storage electrode alloys for nickel–metal hydride batteries. J Power Sources 2004;129(2):358–67.

[20] Liu Yongfeng, Pan Hongge, Gao Mingxia, Zhu Yunfeng, Lei Yongquan, Wang Qidong. Electrochemical studies on $La_{0.7}Mg_{0.3}Ni_{3.4-x}Co_{0.6}Mn_x$ metal hydride electrode alloys. Mater Chem Phys 2004;84(1):171–81.

[21] Liu Yongfeng, Pan Hongge, Gao Mingxia, Zhu Yunfeng, Lei Yongquan, Wang Qidong. The effect of Mn substitution for Ni on the structural and electrochemical properties of $La_{0.7}Mg_{0.3}Ni_{2.55-x}Co_{0.45}Mn_x$ hydrogen storage electrode alloys. Int J Hydrogen Energy 2004;29(3):297–305.

[22] Joubert JM, Latroche M, Percheron-Guégan A, Bourée-Vigneron F. Thermodynamic and structural comparison between two potential metal-hydride battery materials $LaNi_{3.55}Mn_{0.4}Al_{0.3}Co_{0.75}$ and $CeNi_{3.55}Mn_{0.4}Al_{0.3}Co_{0.75}$. J Alloys Compd 1998;275–277:118–22.

[23] Paul-Boncour V, Joubert JM, Latroche M, Percheron-Guégan A. In situ XAS study of the hydrogenation of AB_5 compounds (A = La, Ce and B = $Ni_{3.55}Mn_{0.4}Al_{0.3}Co_{0.75}$). J Alloys Compd 2002;330–332:246–9.

[24] Qingxue Zeng, Joubert JM, Latroche M, Jun Du, Percheron-Guégan A. Influence of the rare earth composition on the properties of Ni–MH electrodes. J Alloys Compd 2003;360(1–2):290–3.

[25] Tliha M, Mathlouthi H, Lamloumi J, Percheron-guegan A. Electrochemical kinetic parameters of a metal hydride battery electrode. Int J Hydrogen Energy 2007;32(5):611–4.

[26] Merzouki A, Cachet-Vivier C, Vivier V, Nédélec JY, Yu LT, Haddaoui N, et al. Microelectrochemistry study of metal-hydride battery materials: cycling behavior of $LaNi_{3.55}Mn_{0.4}Al_{0.3}Co_{0.75}$ compared with $LaNi_5$ and its mono-substituted derivatives. J Power Sources 2002;109(2):281–6.

[27] Tan Zuxian, Yang Yifu, Li Yan, Shao Huixia. The performances of $La_{1-x}Ce_xNi_5$ ($0 \le x \le 1$) hydrogen storage alloys studied by powder microelectrode. J Alloys Compd 2008;453(1–2):79–86.